Optimal Operation of Energy Storage to Minimize Wind Spillage and Mitigate Wind Power Forecast Errors

Hamideh Bitaraf, *Student Member, IEEE*, Saifur Rahman, *Fellow, IEEE*

***Abstract*— Wind spill occurs due to the non-correlation between load and wind profiles, and also wind power forecast errors. Scheduling energy storage units to reduce wind spillage gets complicated considering the difference between day-ahead wind power forecast range, hour-ahead wind power forecast, and actual wind power. This paper presents an algorithm that optimally schedules energy storage to address both applications - minimizing wind spillage and mitigating wind power forecast errors. First, energy storage is scheduled to minimize wind spillage by a mixed integer linear programming, given day-ahead wind power forecast range. Then, day-ahead energy storage operation is updated to mitigate the error between day-ahead wind power forecast and hour-ahead wind power forecast, using Discrete Wavelet Transform (DWT). Finally, energy storage operation is updated by DWT to mitigate the error between actual wind power and hour-ahead wind power forecast. Wind spillage and required back-up generation is calculated for different scenarios of day-ahead wind power forecast, energy storage technologies (e.g. compressed air energy storage, and sodium sulfur battery), and state of charge values. To showcase the applicability of the proposed approach, a case study based on the real world wind and load data obtained from the Bonneville Power Administration in 2013 is presented.**

***Index Terms*—Wind spillage, wind power forecast errors, compressed air energy storage, sodium sulfur battery, energy storage operation, mixed integer linear programming, Discrete Wavelet Transform.**

I. Introduction

Wind spillage occurs due to the non-correlation between wind and load profiles at high wind energy penetration levels. When wind power exceeds load minus must-run generation (e.g. nuclear and thermal power plants), the unusable wind generation has no option but curtailment. Large-scale energy storage units can be operated to minimize this wind spillage. This problem gets complicated because the day-ahead wind power is forecasted in a range identified by maximum, average, and minimum quantities. On the other hand, there is always some error between day-ahead wind power forecast range, hour-ahead wind power forecast, and actual wind generation.

In the literature, sizing of energy storage units is solved in [3]-[8] to maximize the revenue or smooth the output power. Energy storage sizing to allow the combined wind and storage output to meet the predicted power output has been addressed in [9]-[12]. Variety of heuristic methods [13]-[14] and Game Theory approaches [15]-[16] have been used to solve energy storage sizing problem in a system with high wind penetration. Sizing energy storage based on pre-compensation and post-compensation to minimize hourly wind forecast error energy is studied in [17]. Sizing batteries is studied in [18] by statistical analysis of wind forecast error.

Energy storage sizing and operation is also solved by signal processing techniques because efficient operation of energy storage or conventional units depends on their cycling. This concept was proposed in [19] to mitigate wind power forecast error. Signal processing techniques were used in planning energy storage and diesel generator to supply load in [20] and to smooth out wind fluctuation in [21].

Authors proposed a method using signal processing techniques (e.g. Discrete Wavelet Transform (DWT)), to mitigate errors between hour-ahead wind power forecast and actual wind power by scheduling Sodium Sulfur (NaS) battery and compressed air energy storage (CAES) [22]. Detailed modeling of NaS battery and CAES to maximize wind energy penetration level was presented by authors in a mixed integer linear programming (MILP) using actual wind power [3].

This paper is upgraded and expanded version of [22] and [3] by presenting a combined algorithm. Contributions and novelties of this paper are summarized as follows.

- Present an algorithm for optimal operation of energy storage that addresses both applications – minimizing wind spillage and mitigating wind forecast errors, in three steps. First, schedule energy storage day-ahead to minimize wind spillage due to non-correlation between load profile and day-ahead wind power forecast range by MILP. Then, update energy storage operation by DWT to mitigate errors between day-ahead wind power forecast, hour-ahead wind power forecast, and actual wind power in two steps.
- Compare final wind spillage and back-up generation for different energy storage units when their operation is not updated, with the case that their operation is updated based on the proposed algorithm.
- Compare final wind spillage and back-up generation when different day-ahead wind power forecast scenarios (e.g. maximum, average, and minimum values) are used to schedule energy storage units for day-ahead operation.
- Compare the impact of refilling energy storage units to different final state of charge values on reducing wind spillage and back-up generation.

This work was supported in part by the U.S. National Science Foundation under grant OISE-1104023.

H. Bitaraf is with Virginia Tech – Advanced Research Institute, Arlington, VA 22203 USA (e-mail: bhamideh@vt.edu).

S. Rahman is professor and director of Virginia Tech – Advanced Research Institute, Arlington, VA 22203 USA (e-mail: srahman@vt.edu).

978-1-5090-4168-8/16/$31.00 ©2016 IEEE

The rest of the paper is organized as follows. Section II describes the scheduling algorithm. Case studies and discussions are presented in section III.

II. Energy Storage Scheduling Algorithm

This paper presents an algorithm to schedule energy storage units in three steps as shown in Fig.1. The algorithm runs for each day, first energy storage units are scheduled based on day-ahead wind power forecast by MILP to minimize wind spillage. Then, their scheduling is updated in two steps using DWT based on the error between day-ahead, and hour-ahead wind power forecast, and actual wind power. The input for each step besides related wind power is the energy storage operation and initial state of charge from previous step. In this algorithm, final state of charge (SoC^f) is given as initial state of charge (SoC^{n-1}) for next day. N_{total}, SoC^i, and n represent total number of days, initial state of charge for first day, and day number, respectively. Three steps of this algorithm are defined as follows.

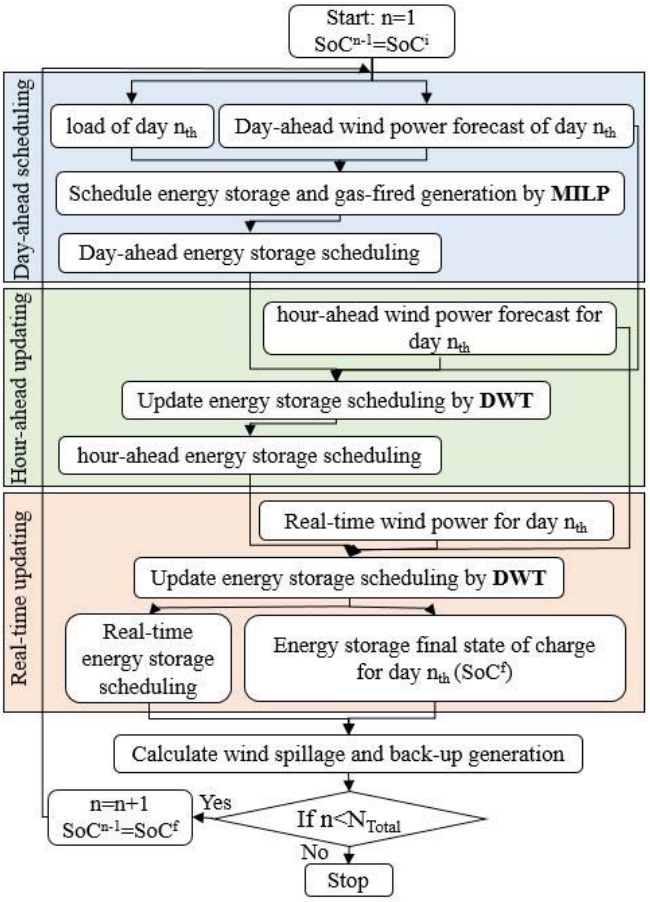

Fig. 1. Energy storage scheduling algorithm

Step 1) *Day-ahead scheduling:*

The mixed integer linear programming (MILP) defined in [22] to model CAES, NaS battery, and gas-fired generation is used in this paper with following four differences.

1) The objective function is to minimize wind spillage:

$$Min \quad \sum_{t=1}^{T} p_{ws,t} \tag{1}$$

Where,

$p_{ws,t}$: Wind spill power at time t

T : Simulation time horizon (for a day)

t : Time interval index (every 5-minute)

2) Day-ahead wind power forecast ($p_{dwf,t}$) is used instead of actual wind power in the power balance constraint. This constraint ensures that the total generation, equals to total load, at each time interval.

3) Energy capacity constraint: This constraint is modified from [22], because energy storage units are scheduled day-ahead, then updated in hour-ahead, and real-time to mitigate wind power forecast. Hence, the initial state of charge at the beginning of next day equals to the previous day final state of charge after updating, which is not constant anymore.

$$0 \le \frac{\sum_{t'=1}^{k} (p_{chg,t'}\eta - p_{dchg,t'})\Delta t}{EN} + SOC^{n-1} \le 1, k = 1 \cdots T \tag{2}$$

Where,

$p_{dchg,t}$: Discharge power at time t

$p_{chg,t}$: Charge power at time t

η : Efficiency

Δt : Time interval

SoC^{n-1} : Initial state of charge

E : Rated energy capacity of energy storage

N : Number of energy storage units

4) Refill constraint: This is modified from [22] and implies that energy storage state of charge is back to desired state of charge at the end of each simulation time horizon, rather than be the same as initial state of charge.

$$\frac{\sum_{t'=1}^{T} (p_{chg,t'}\eta - p_{dchg,t'})\Delta t}{EN} + SOC^{n-1} = SOC^{df} \tag{3}$$

Where,

SoC^{df} : Desired final state of charge

Step 2) *Hour-ahead updating:*

DWT method proposed in [23] is used to decompose the error between day-ahead and hour-ahead wind forecast powers for scheduling CAES, and NaS battery. First, the error signal is derived as shown in (4).

$$p_{fe1,t} = p_{dwf,t} - p_{hwf,t}, \forall t \tag{4}$$

Where,

$p_{fe1,t}$: Error between day-ahead and hour-ahead wind forecast powers at time t

$p_{dwf,t}$: Day-ahead wind power forecast at time t

$p_{hwf,t}$: Hour-ahead wind power forecast at time t

Then, high, medium, and low frequency components are derived by using DWT method. The difference between this paper and method proposed in [23] are defined below.

First, energy storage units are prescheduled by day-ahead wind power forecast, rather than only be used for mitigating forecast error. This modifies the control signal of energy storage units which are shown in (5) and (6) for CAES and

978-1-5090-4168-8/16/$31.00 ©2016 IEEE

NaS battery, respectively. As shown in (5), CAES control signal is CAES day-ahead scheduling plus medium frequency component of the error signal derived in (4).

$$p_{C,t} = (p_{Cdchg,t} - p_{Cchg,t}) + p_{mf,t}, \forall t \quad (5)$$

Where,

$p_{C,t}$: CAES control signal at time t in MW.

$p_{mf,t}$: Medium frequency component at time t

$p_{Cchg,t}$: CAES charge power derived from step1

$p_{Cdchg,t}$: CAES discharge power derived from step1

Then this control signal (5) is the new input to the algorithm proposed in [23] that applies CAES properties such as power and energy limits, ramp rate, and required idle time at each time interval. The output is CAES operation ($p_{CAES,t}$).

Then, NaS battery control signal is the summation of its day-ahead scheduling plus high frequency component and also the difference between CAES operation and its initial control signal as shown in (6).

$$p_{N,t} = (p_{Ndchg,t} - p_{Nchg,t}) + p_{hf,t} + (p_{CAES,t} - p_{C,t}), \forall t \quad (6)$$

Where,

$p_{N,t}$: NaS control signal at time t in MW.

$p_{hf,t}$: High frequency component at time t

$p_{Nchg,t}$: NaS charge power derived from step1

$p_{Ndchg,t}$: NaS discharge power derived from step1

Then this control signal (6) is the new input to the algorithm proposed in [23] that applies NaS battery properties such as power limit, energy capacity limit, and state of charge limit. The output is NaS operation ($p_{NaS,t}$).

Step 3) *Real-time updating:*

This step is the same as step 2, with following differences. First, the error signal is the difference between hour-ahead wind power forecast and actual wind power as (7).

$$p_{fe2,t} = p_{hwf,t} - p_{aw,t}, \forall t \quad (7)$$

Where,

$p_{fe2,t}$: Error between hour-ahead and actual wind power at time t

$p_{aw,t}$: Actual wind power at time t

Second, the energy storage control signal is the summation of energy storage scheduling derived from step 2 and the related decomposed component of error signal in (7) by DWT. Finally the last state of charge for energy storage units is extracted from this third step and given as the input for the next day.

Step 4) *calculating final wind spillage and back-up generation*

The residual power is calculated as shown in (8), which equals to the total generation (inflexible generation, thermal units, energy storage discharging power, wind power, and low-frequency component) minus total load (load, and energy storage charging power) at each time interval.

$$p_{residual,t} = P_{ig} + p_{aw,t} + p_{gf,t} + p_{dchg,t} - p_{chg,t} + p_{lf,t} - p_{l,t}, \forall t \quad (8)$$

Where,

$p_{residual,t}$: Residual power at time t

P_{ig} : Inflexible (must-run) generation

$p_{gf,t}$: Gas-fired generation at time t

$p_{lf,t}$: Low frequency components derived from DWT of step 2 and step 3

$p_{l,t}$: Load at time t

Wind spillage and back-up generation are the positive and negative quantities of this residual signal, respectively.

III. Case Studies and Discussions

To showcase the applicability of the proposed approach, different case studies based on wind and load data with 5-minute interval, obtained from the Bonneville Power Administration (BPA) in 2013 [24] are investigated. BPA day-ahead wind power is forecasted in a range identified by maximum, average, and minimum values as shown Fig. 2. The hour-ahead wind power forecast and actual wind power are also depicted in Fig. 2 for the same day. This figure show the problem addressed by the proposed algorithm that mitigates errors between day-ahead forecast, hour-ahead forecast and actual wind power while energy storage units are scheduled based on day-ahead wind power forecast at its first step.

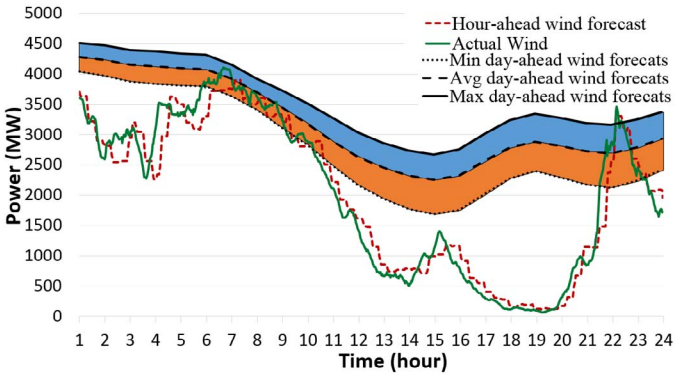

Fig. 2. A day in BPA 2013 showing actual wind generation, hour-ahead wind power forecast, and day-ahead wind power forecast range.

BPA peak load in 2013 is 10.6 GW, and installed wind capacity is 4.5 GW. Wind energy penetration is 20% in BPA, while neglecting net interchange. Nuclear generation and gas-fired generation are considered in this paper to be able to provide 100% of annual peak load to guarantee system reliability. Nuclear generation is considered to be a must-run generation providing 20% of peak load with 95% availability. Hence, nuclear must-run power is 2 GW. Gas-fired generation parameters are shown in Table I. Modeling parameters for energy storage technologies including CAES and NaS battery are presented in Table II.

TABLE I
GAS-FIRED GENERATION PARAMETERS[25]

Capacity (GW)	9
Min Stable Generation (%)	20
Ramp up/down (% of installed capacity per min)	8
Min up/down Time (hours)	2

TABLE II
LARGE-SCALE ENERGY STORAGE PARAMETERS [26], [27]

Energy Storage Technology	CAES	NaS
Power Capacity (MW)	300	50
Energy Capacity (MWh)	6000	300
Ramp Rate (MW/min)	18	---
Efficiency (%)	70	75
Required Idle Time to Switch Modes (min)	20	---
Max and Min State of Charge	1,0	0.9,0.1

Different case studies are investigated by simulating BPA data for one month (April) in 2013 with 5-minute time interval. Characteristics of errors between maximum, average, minimum day-ahead wind power forecasts, and hour-ahead wind power forecast with actual (real-time) wind power is extracted and shown in Table III. As shown, if energy storage units are only used for day-ahead scheduling, extra energy storage units are required to be installed for mitigating this error.

TABLE IIII
WIND POWER FORECAST ERRORS

	Mean (MW)	Sigma (MW)	Max (MW)	Min (MW)
Actual wind minus maximum day-ahead wind forecast	-317	1131	3782	-3836
Actual wind minus average day-ahead wind forecast	-12	1121	3891	-3609
Actual wind minus minimum day-ahead wind forecast	310	1130	3974	-3374
Actual wind minus hour-ahead wind forecast	34	236	1225	-1316

Proposed algorithm updates day-ahead energy storage operation to be able to mitigate wind power forecast errors. The results of this algorithm for final wind spillage and back-up generation for different energy storage technologies, and different day-ahead wind power forecast ranges are shown in Fig.3 and Fig.4, respectively. As shown, CAES operation based on maximum day-ahead wind forecast results in 250 GWh more wind spillage and 140 GWh less back-up generation as compared to energy storage operation based on average one. This is a tradeoff between scheduling based on different scenarios of day-ahead wind power forecasts that higher day-ahead wind power forecast results in more wind spillage but less required back-up generation.

As shown in Fig. 3 and Fig.4, three different desired final state of charges (SoC) for refilling energy storage units at the end of each day are also simulated. Updating CAES based on refillig to 20% SoC results in 16 GWh and 75 GWh less wind spillage as compared to 50% and 80% state of charge scenarios, respectively. On the other hand, case study based on 20% SoC results in 33 GWh and 9 GWh more back-up generation as compared to 50% and 80% state of charge scenarios, respectively based on maximum day-ahead wind power forecast scheduling.

The differences between updating energy storage scheduling for different scenarios of day-ahead wind power forecast values, desired final SoC quantities, and energy storage technologies, with the base case scenario, which is not updating day-ahead energy storage operation are shown in Table IV.

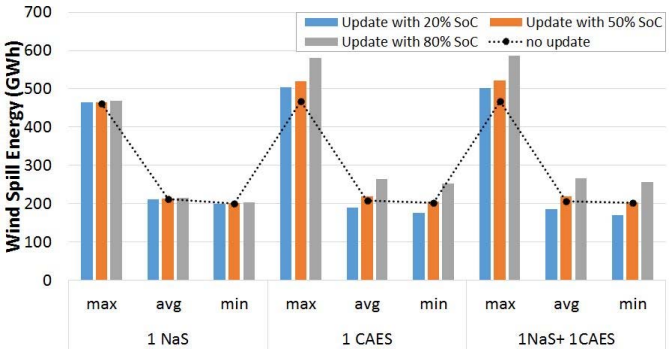

Fig. 3. Final wind spillage based on different scenarios

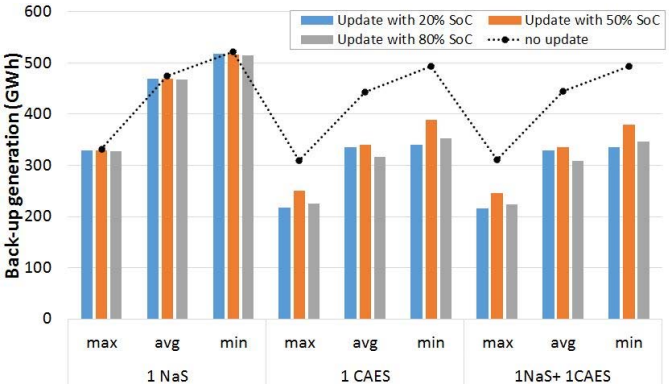

Fig. 4. Final back-up generation based on different scenarios

TABLE IV
REDUCTION IN WIND SPILLAGE AND BACK-UP GENERATION AS COMPARED TO BASE CASE SCENARIO

SoC		20%		50%		80%	
		Wind spill reduction	Back-up reduction	Wind spill reduction	Back-up reduction	Wind spill reduction	Back-up reduction
NaS	Max	-1.5	3.1	-3.4	3.7	-5.4	4.6
	Avg	0.4	4.9	-0.8	6.1	-2.9	6.7
	Min	0.2	4.4	-1.3	5.4	-3.2	6.4
CAES	Max	-37.6	92.5	-52.6	59.5	-112.5	83.6
	Avg	17.9	108.2	-10.9	103.2	-56.7	126.7
	Min	26.6	152.2	-3.5	104.5	-50.0	140.0
NaS + CAES	Max	-34.4	95.0	-54.8	64.6	-119.7	87.4
	Avg	20.5	116.4	-11.1	109.9	-59.2	136.5
	Min	32.5	157.6	-1.0	114.3	-53.5	147.9

Negative and positive values shown in Table IV presents increase and decrease as compared to base case (no updating scenario), respectively. As shown, all back-up generation values are positive, stating the fact that updating based on proposed algorithm reduces the amount of required back-up generation for mitigating wind power forecats errors. But, wind spillage has both positive and negative values. Fore example, if CAES operation is updated, it reduces wind spillage by 26GWh and back-up generation by 152 GWh for scheduling based on minimum day-ahead wind forecast with 20% SoC refill. But, when CAES is refilled to 80% SoC for the same scenario, wind spillage is increased by 50 GWh and back-up generation is reduced by 140 GWh. On the other hand, if maximum day-ahead wind power forecast values are used to schedule CAES for 20% SoC refill, then wind spillage is increased by 37.6 GWh and back-up generation is decreased by 92.5 GWh.

978-1-5090-4168-8/16/$31.00 ©2016 IEEE

IV. Conclusion

This paper presents an algorithm to optimally operate energy storage units based on the day-ahead wind power forecast and then update it to mitigate wind forecast errors. This scheduling addresses both high wind energy penetration challenges - wind spillage and wind power forecast error.

Tradeoffs between different case studies such as energy storage technologies, using maximum, average, and minimum day-ahead wind power forecast values, refilling to various states of charge amounts, are investigated on final wind spillage and back-up generation required. Refilling to lower state of charge, more energy storage technologies, and using minimum day-ahead wind power forecast have a better overall results in terms of lower wind spillage and back-up generation as compared to the case when energy storage is not updated. This algorithm reduces the need to install more energy storage units by updating energy storage operation based on wind forecast error signals.

References

[1] L. Fried, S. Sawyer, S. Shukla, and L. Qiao, "Global wind report: Annual market update 2013," GWEC [Online]. Available: gwec.net/wp-content/uploads/2014/04/GWEC-Global-Wind-Report_9-April-2014.pdf

[2] P. Meibom, K.B. Hilger, H. Madsen, D. Vinther, "Energy Comes Together in Denmark: The Key to a Future Fossil-Free Danish Power System," *IEEE Power and Energy Magazine*, vol.11, no.5, pp.46-55, Sept.-Oct. 2013

[3] H. T. Le, S. Santoso, and T. Q. Nguyen, "Augmenting wind power penetration and grid voltage stability limits using ESS: application design, sizing, and a case Study," *IEEE Trans. on Power Systems,* vol. 27, no. 1, pp. 161-171, Feb. 2012.

[4] C. Abbey, and G. Joos, "A stochastic optimization approach to rating of energy storage systems in wind-diesel isolated grids," *IEEE Trans. on Power Systems,* vol. 24, no. 1, pp. 418-426, Apr. 2009.

[5] Y. Levron, J. M. Guerrero, and Y. Beck, "Optimal power flow in micro grids with energy storage," *IEEE Trans. on Power Systems*, vol. 28, no. 3, pp. 3226-3234, Apr. 2013.

[6] D. Gayme, and U. Topcu, "Optimal power flow with large-scale storage integration," *IEEE Trans. on Power Systems*, vol. 28, no. 2, pp. 709-717, May. 2013.

[7] S. Teleke, M. E. Baran, S. Bhattacharya, and A. Q. Huang, "Rule-based control of battery energy storage for dispatching intermittent renewable sources," *IEEE Trans. on Sustainable Energy,* vol. 1, no. 3, pp. 117-124, Oct. 2010.

[8] L. Xu, X. Ruan, Ch. Mao, B. Zhang and Y. Luo, "An Improved Optimal Sizing Method for Wind-Solar-Battery Hybrid Power System," *IEEE Trans. on Sustainable Energy*, vol. 4, no. 3, pp. 774-785, July. 2013.

[9] T. K. A. Brekken, A. Yokochi, A. V. Jouanne, Z. Z. Yen, H. M. Hapke, and D. A. Halamay, "Optimal energy storage sizing and control for wind power applications," *IEEE Trans. on Sustainable Energy*, vol. 2, no. 1, pp. 69-77, Jan. 2011

[10] S. Teleke, M. E. Baran, A. Q. Huang, S. Bhattacharya, and L. Anderson, "Control strategies for battery energy storage for wind farm dispatching," *IEEE Trans. on Energy Conversion.,* vol. 24, no. 3, pp.725-732, Sep. 2009.

[11] P. Wang, Z. Gao, and L. Bertling, "Operational adequacy studies of power systems with wind farms and energy storages," *IEEE Trans. on Power Systems*, vol. 27, no. 4, pp. 2377-2384, Nov. 2012.

[12] C. Wang, Z. Lu, and Y. Qiao, "A consideration of the wind power benefits in day-ahead scheduling of wind-coal intensive power systems," *IEEE Trans. on Power Systems*, vol. 28, no. 1, pp. 236-245, Feb. 2013.

[13] M. Ghofrani, A. Arabali, M. Etezadi-Amoli and M. S. Fadali, "Energy Storage Application for Performance Enhancement of Wind Integration," *IEEE Trans. on Power Systems*, vol. 28, no. 4, pp. 4803-4811, Nov. 2013.

[14] S. Teleke, M. E. Baran, S. Bhattacharya, and A. Q. Huang, "Rule-based control of battery energy storage for dispatching intermittent renewable sources," *IEEE Trans. on Sustainable Energy*, vol. 1, no. 3, pp. 117-124, Oct. 2010.

[15] S. Mei, Y. Wang, F. Liu, X. Zhang, and Z. Sun, "Game Approaches for Hybrid Power System Planning," *IEEE Trans. on Sustainable Energy*, vol. 3, no. 3, pp. 506-517, July. 2012.

[16] Sh. Mei, D. Zhang, Y. Wang, F. Liu, and W. Wei, "Robust Optimization of Static Reserve Planning With Large-Scale Integration of Wind Power: A Game Theoretic Approach," *IEEE Trans. on Sustainable Energy*, vol. 5, no. 2, pp. 535-545, April. 2014.

[17] Ke, X.; Lu, N.; Jin, C., "Control and Size Energy Storage Systems for Managing Energy Imbalance of Variable Generation Resources," *IEEE Trans. on Sustainable Energy*, vol.6, no.1, pp.70, 78, Jan. 2015.

[18] Luo, F.; Meng, K.; Dong, Z.Y.; Zheng, Y.; Chen, Y.; Wong, K.P., "Coordinated Operational Planning for Wind Farm With Battery Energy Storage System," *IEEE Trans. on Sustainable Energy*, vol.6, no.1, pp.253,262, Jan. 2015.

[19] Y. V. Makarov, P. Du, M. C. W. Kintner-Meyer, J. Chunlian, and H. F. Illian, "Sizing energy storage to accommodate high penetration of variable energy resources," *IEEE Trans. on Sustainable Energy*, vol. 3, no. 1, pp. 34-40, Jan. 2012.

[20] J. Xiao, L. Bai, F. Li, H. Liang and C. Wang, "Sizing of Energy Storage and Diesel Generators in an Isolated Microgrid Using Discrete Fourier Transform (DFT)," *IEEE Trans. on Sustainable Energy*, vol. 5, no. 3, pp. 907-916, July. 2014.

[21] Q. Jiang, and H. Hong, "Wavelet-based capacity configuration and coordinated control of hybrid energy storage system for smoothing out wind power fluctuations," *IEEE Trans. on Power Systems*, vol. 28, no. 2, pp. 1363-1372, May. 2013

[22] H. Bitaraf, S. Rahman, M. Pipattanasomporn, "Sizing Energy Storage to Mitigate Wind Power Forecast Error Impacts by Signal Processing Techniques," *IEEE Trans. on Sustainable Energy,* vol.6, no.4, pp.1457-1465, Oct. 2015

[23] H. Bitaraf, H. Zhong, and S. Rahman, "Managing Large Scale Energy Storage Units to Mitigate High Wind Penetration Challenges", *IEEE Power and Energy Society General Meeting*, 5p, 22-26 July 2015, Denver, Colorado.

[24] Historical data 2013. [Online]. Available: transmission.bpa.gov/Business/operations/Wind/default.aspx

[25] I. Perez-Arriaga: *Managing Large Scale Penetration of Intermittent Renewables*, MITEI Symposium on Managing Large-Scale Penetration of Intermittent Renewables, Cambridge, U.S.A, 20 April 2011, 43p.

[26] F. S. Barnes, J. G. Levine, *Large scale energy storage handbook*, by CRC Press, March 3, 2011.

[27] R. Carnegie, D. Gotham, D. Nderitu, P. V. Preckel, *Utility Scale Energy Storage Systems, Benefits, Application, and Technologies,* by State Utility Forecasting Group, June 2013 [Online]. Available: purdue.edu/discoverypark/energy/assets/pdfs/SUFG/publications/SUFG%20Energy%20Storage%20Report.pdf

Biography

Hamideh Bitaraf (S'11) received her B.S. and M.S. degrees from Electrical Engineering Department of Sharif University of Technology, Tehran, Iran, in 2010 and 2012 respectively. She is currently working toward the Ph.D. degree in Bradley Department of Electrical and Computer Engineering at Virginia Polytechnic and state university. She is a graduate research assistant at Virginia Tech – Advanced Research Institute Arlington, VA, USA, since 2012. Her research interests include energy storage, wind power, demand response, renewable energy, and smart grid, signal processing and optimization methods.

Saifur Rahman (S'75-M'78-SM'83-F'98) is the director of the Advanced Research Institute at Virginia Tech, Arlington, VA, USA, where he is the Joseph Loring Professor of electrical and computer engineering. He also directs the Center for Energy and the Global Environment at the university. In 2014 he is serving as the editor-in-chief of the IEEE Electrification Magazine. Prof. Rahman served as the chair of the U.S. National Science Foundation Advisory Committee for International Science and Engineering from 2010 to 2013. In 2006 he served as the vice president of the IEEE Publications Board, and a member of the IEEE Board of Governors. He is a distinguished lecturer of IEEE PES, and has published in the areas of smart grid, energy efficiency, conventional and renewable energy systems, load forecasting, uncertainty evaluation, and infrastructure planning.

978-1-5090-4168-8/16/$31.00 ©2016 IEEE